2009-11

Photoluminescence property of Ba('Zr IND.0.25''Ti IND.0.75)'O IND.3' powders prepared by solid state reaction and polymeric precursor method

Physica B,Amsterdam,v. 404, n. 20, p. 3341-3347, Nov. 2009
http://www.producao.usp.br/handle/BDPI/49377

Physica B 404 (2009) 3341–3347

Contents lists available at ScienceDirect

Physica B

journal homepage: www.elsevier.com/locate/physb

Photoluminescence property of $Ba(Zr_{0.25}Ti_{0.75})O_3$ powders prepared by solid state reaction and polymeric precursor method

S.K. Rout [a], L.S. Cavalcante [b,*], J.C. Sczancoski [b], T. Badapanda [c], S. Panigrahi [c], M. Siu Li [d], E. Longo [b]

[a] Department of Applied Physics, BIT, Mesra, Ranchi, Jharkhan 835-215, India
[b] DQ-UFSCar e UNESP, P.O. Box 355, 14801-907, São Carlos e Araraquara, SP, Brazil
[c] Department of Physics, NIT, Rourkela, Orissa 769 008, India
[d] Instituto de Física de São Carlos, USP, P.O. Box 369, 13560-970, São Carlos, SP, Brazil

ARTICLE INFO

Article history:
Received 2 April 2009
Accepted 12 May 2009

PACS:
77.84.Dy
74.62.Bf
71.23.An
78.55.−m

Keywords:
Ceramics
Crystal structure
Localized states
Photoluminescence

ABSTRACT

$Ba(Zr_{0.25}Ti_{0.75})O_3$ (BZT) powders were synthesized by the polymeric precursor method (PPM) at different temperatures (400, 500 and 700 °C) for 2 h and by the solid state reaction (SSR) at 1350 °C for 4 h. These powders were analyzed by X-ray diffraction (XRD), ultraviolet–visible (UV–vis) absorption spectroscopy and photoluminescence (PL) measurements. XRD patterns indicated that the crystalline BZT powders prepared by both methods present a cubic structure. The different optical band gap values were observed from the UV–vis spectra, suggesting the presence of intermediary energy levels (shallow and deep holes) within the band gap. When excited with 350 nm wavelength at room temperature, the BZT powders obtained by SSR exhibited only one broad PL band with a maximum at around 467 nm (blue emission). On the other hand, it was noted the presence of two broad bands when BZT powders were prepared by the PPM, where the correspondent positions are influenced by the heat treatment temperatures. Finally, a model was proposed in order to explain the origin of the PL property in these powders.

1. Introduction

In the last years, Pb-based ceramic oxides have been widely studied due to its excellent ferroelectric, dielectric and piezoelectric properties [1–3]. In particular, $PbTiO_3$-based solid solutions have dominated for decades the technological field responsible for the development of piezoelectric materials [4]. However, these materials present two serious drawbacks when heat treated in range from 500 to 900 °C [5], i.e., the volatility and toxicity involved with the Pb [6]. Thus, the scientific community has searched new materials with interesting chemical and physical properties in order to replace the Pb-based compounds for environmental friendly applications [7]. An alternative material for this purpose is $Ba(Zr,Ti)O_3$ (BZT) [8–14], which has important applications in microwave technologies because of its high dielectric constant, low dielectric loss and large tunability when compared to the $(Ba,Sr)TiO_3$ ceramics [15,16]. The electrical properties exhibited by this material are arising from a lattice expansion effect because that the ionic radii of Zr (0.087 nm) is higher and more stable than the Ti (0.068 nm) [17,18]. In principle, different factors are able to influence in the dielectric and ferroelectric properties of this material, such as: average grain size distribution, sintering temperature, presence of dopant ions (La^{3+}, Pr^{3+}, Nd^{3+}, Dy^{3+}, Er^{3+}, Nb^{5+}, Bi^{3+}, V^{5+}, W^{5+}) and/or composites (MgO) into the matrix [19–25].

Currently, several synthesis methods have been employed to obtain BZT powders or thin films, for example: hydrothermal process from peroxo-precursors [26], aqueous co-precipitation technique [27], sol–gel [28] and sol–gel–ethanol thermal method [29]. Although these methods have shown potential in the preparation of pure BZT phase at low temperatures, they are not able to improve the electrical properties due to the formation of small particle sizes. On the other hand, the solid state reaction (SSR) promotes a grain growth process in these ceramic oxides, resulting in good dielectric, piezoelectric, tunability and ferroelectric properties [30–32].

In terms of optical properties, some studies of crystalline and non-crystalline BZT materials reported in the literature has mainly focused on the infrared optical properties, complex refractive index and photoluminescence (PL) emissions [33–37]. Therefore, in this letter, we report on the photoluminescence properties at room temperature of $Ba(Zr_{0.25}Ti_{0.75})O_3$ (BZT) powders prepared by the polymeric precursor method (PPM) at different temperatures

* Corresponding author. Tel.: +55 16 3361 5215; mobile: +55 16 9176 49 43.
E-mail address: laeciosc@bol.com.br (L.S. Cavalcante).

0921-4526/$ - see front matter © 2009 Elsevier B.V. All rights reserved.
doi:10.1016/j.physb.2009.05.014

(400, 500 and 700 °C) for 2 h and by the SSR at 1350 °C for 4 h. These powders were analyzed by X-ray diffraction (XRD), ultraviolet–visible (UV–vis) absorption spectroscopy and photoluminescence measurements.

2. Experimental procedure

2.1. Synthesis of $Ba(Zr_{0.25}Ti_{0.75})O_3$ powders by solid state reaction and polymeric precursor method

In the SSR, $BaCO_3$ (99.9%, S.D. Fine Chem., Mumbai), TiO_2 (99.9% E. Merck India Ltd.) and ZrO_2 (99.9% Loba Chem., Mumbai) were used as raw materials. These powders were stoichiometric mixed using isopropyl alcohol (IPA) and milled by means of an agate mortar to obtain a homogeneous powder. Afterwards, this powder was heat treated at 1300 °C for 6 h with repeated cycles of mixing and grinding. Finally, the pure BZT phase was obtained when the heat treatment was performed at 1350 °C for 4 h.

In the PPM, three samples of BZT powders were prepared using barium nitrate [$Ba(NO_3)_2$] (99.5%, Aldrich), titanium isopropoxide [$Ti(OC_3H_7)_4$] (99%, Sigma-Aldrich), zirconium *n*-propoxide [$Zr(OC_3H_7)_4$] (99%, NOAH Technologies), ethylene glycol ($C_2H_6O_2$) (99.5% J.T. Baker), citric acid ($C_6H_8O_7$) (99.5%, Mallinckrodt) as raw materials. In a typical experimental procedure, Ti and Zr citrates were formed by the dissolution of [$Ti(OC_3H_7)_4$] and [$Zr(OC_3H_7)_4$] in citric acid aqueous solutions under constant stirring. These solutions were homogenized and mixed with a molar proportion of 25:75 between Zr and Ti, respectively. This citrate solution was stirred and heated at 90 °C to obtain a clear and homogenous solution. In the sequence, $Ba(NO_3)_2$ was dissolved in stoichiometric quantity into the Ti–Zr citrate solution. The solution pH was adjusted to 7 with ammonium hydroxide (NH_4OH) (30%, Mallinckrodt), preventing the precipitation of barium citrate. After solution homogenization, $C_2H_6O_2$ was added in order to promote the citrate polymerization by means of the polyesterification reaction. Into this system, the citric acid/ethylene glycol mass ratio was fixed at 60:40 wt%. The resulting solution was heated at 120 °C under constant stirring to eliminate water, consequently forming a polymeric resin. This polymeric resin was then placed in a conventional furnace and heat treated at 350 °C for 4 h to promote the organic matter decomposition arising from $C_6H_8O_7$ and $C_2H_6O_2$. Finally, the obtained precursors were heat treated at different temperatures (400, 500 and 700 °C) for 2 h.

2.2. Characterizations

BZT powders prepared by SSR and PPM were structurally characterized by X-ray diffraction using a DMax/2500PC diffractometer (Rigaku, Japan). XRD patterns were obtained using Cu-Kα radiation in the 2θ range from 10° to 75° with a scanning rate of 0.02°/min. UV–vis spectra were taken using a Cary 5G (Varian, USA) equipment in diffuse reflection mode. PL measurements were performed through a Monospec 27 monochromator (Thermal Jarrel Ash, USA) coupled to a R446 photomultiplier (Hamamatsu Photonics, Japan). A krypton ion laser (Coherent Innova 90 K, USA) with 350 nm wavelength was used as excitation source, keeping its maximum output power at 200 mW. UV–vis and PL spectra were taken three times for each sample in order to ensure the reliability of the measurements. All measurements were performed at room temperature.

3. Results and discussion

3.1. X-ray diffraction analyses

Figs. 1(a,b) show the XRD patterns of BZT powders prepared by PPM and SSR.

XRD patterns were employed to analysis the structural evolution process at long-range or lattice periodicity during the crystallization process of BZT powders with the increase of heat treatment temperature. In Fig. 1(a), the powders prepared by the PPM and heat treated at 400 °C did not exhibit diffraction peaks ascribed to BZT phase, suggesting a typical behavior of material in amorphous state or disordered at long-range (Fig. 1(a)). However, when the BZT powders were heat treated at 500 °C for 2 h, it was observed the presence of diffraction peaks related to the two

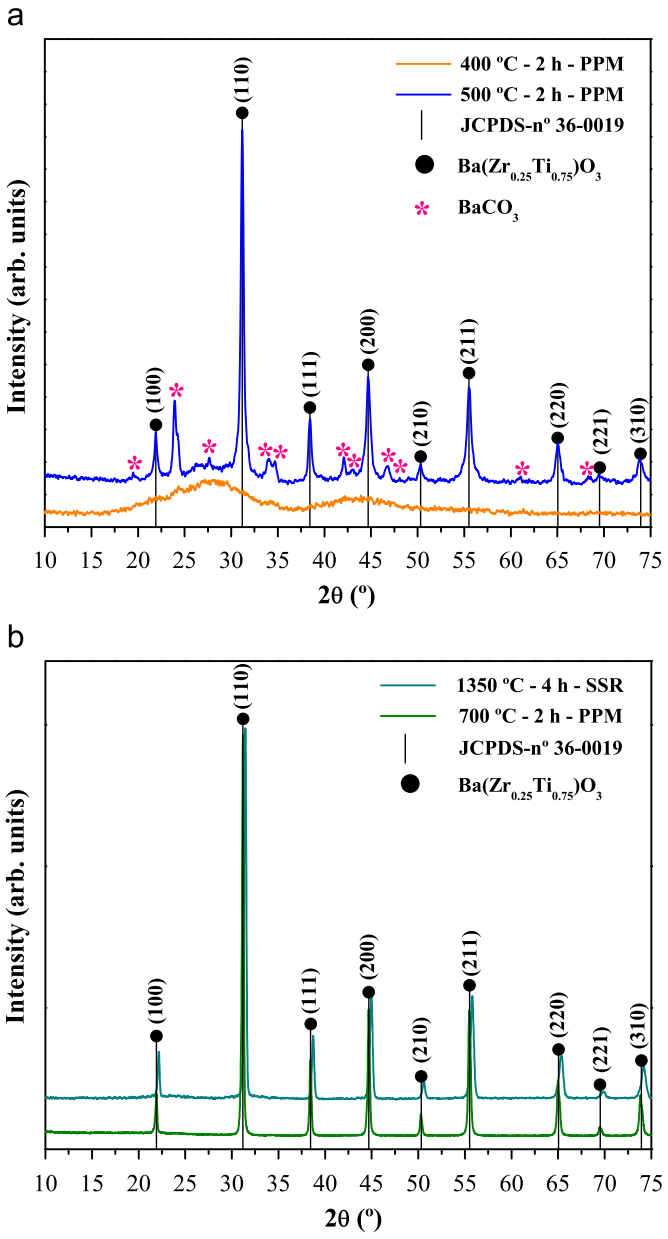

Fig. 1. (a) XRD patterns of BZT powders prepared by PPM and heat treated at 400–500 °C for 2 h and (b) XRD patters of BZT powders prepared by SSR and heat treated at 1350 °C for 2 h and BZT prepared by PPM and heat treated at 700 °C for 2 h. The vertical lines (|) indicate the relative position of JCPDS card no. 36-0019.

different phases (BZT and $BaCO_3$) [38]. Possibly, the formation of the $BaCO_3$ (secondary phase) was caused by the presence of a reductive atmosphere, which is arising from the organic compound decomposition ($C_2H_6O_2$ and $C_6H_8O_7$) into the system. However, the heat treatment performed at 700 °C favored the formation of pure BZT phase (Fig. 1(b)). This result suggests that the increase of heat treatment temperature promotes a decomposition process of the secondary phase ($BaCO_3 \xrightarrow{\triangle} BaO + CO_2$) as well as a structural rearrangement of barium clusters into the BZT lattice. Also, as it can be seen in this figure, the powders prepared by SSR and heat treated at 1350 °C for 4 h presented only diffraction peaks corresponding to pure BZT phase. Probably, the several stages of gridding and heat treatment in this high temperature were key factors in order to promote a slow kinetics of interdiffusion in the contact points between the $BaCO_3$, TiO_2 and ZrO_2 to complete the reaction and to form the final product (BZT phase). Moreover, the XRD patterns of both powders prepared by PPM at 700 °C and SSR at 1350 °C showed intense and well-defined diffraction peaks (Fig. 1(b)), indicating a high degree of structural order at long-range. These diffraction peaks were indexed to the perovskite-type cubic structure with space group $Pm\bar{3}m$, in agreement with the respective "Joint Committee on Powder Diffraction Standards" (JCPDS) card no. 36-0019 [39]. The XRD results obtained in this work are also in agreement with those previously reported in the literature [40,41].

The lattice parameters and unit cell volume of BZT powders prepared by PPM at 700 °C and SSR at 1350 °C were calculated by means of the UNITCELL-97 program [42] and using the regression diagnostics combined with nonlinear least squares to refine cell parameters from powder diffraction data. Table 1 shows a comparison between the lattice parameter values obtained in this work with those reported in the literature [40,41] and JCPDS card [39].

Table 1
Lattice parameter and unit cell volume values of BZT powders prepared by PPM and SSR heat treated at 700 °C for 2 h and 1350 °C for 4 h, respectively.

Method	T (°C)	Time (h)	$a = b = c$ lattice parameter (Å)	Unit cell volume (Å^3)	Ref.
SSR	1400	6	4.06	66.923(4)	[40]
SSR	1400	6	4.04	65.939(2)	[40]
PPM	700	2	4.0502	66.439(9)	[41]
SSR	1350	4	4.0493(4)	66.397(8)	[⊛]
PPM	700	2	4.0527(7)	66.566(4)	[⊛]
JCPDS			4.05	66.528(5)	[39]

T = temperature, Ref. = references and [⊛] = this work.

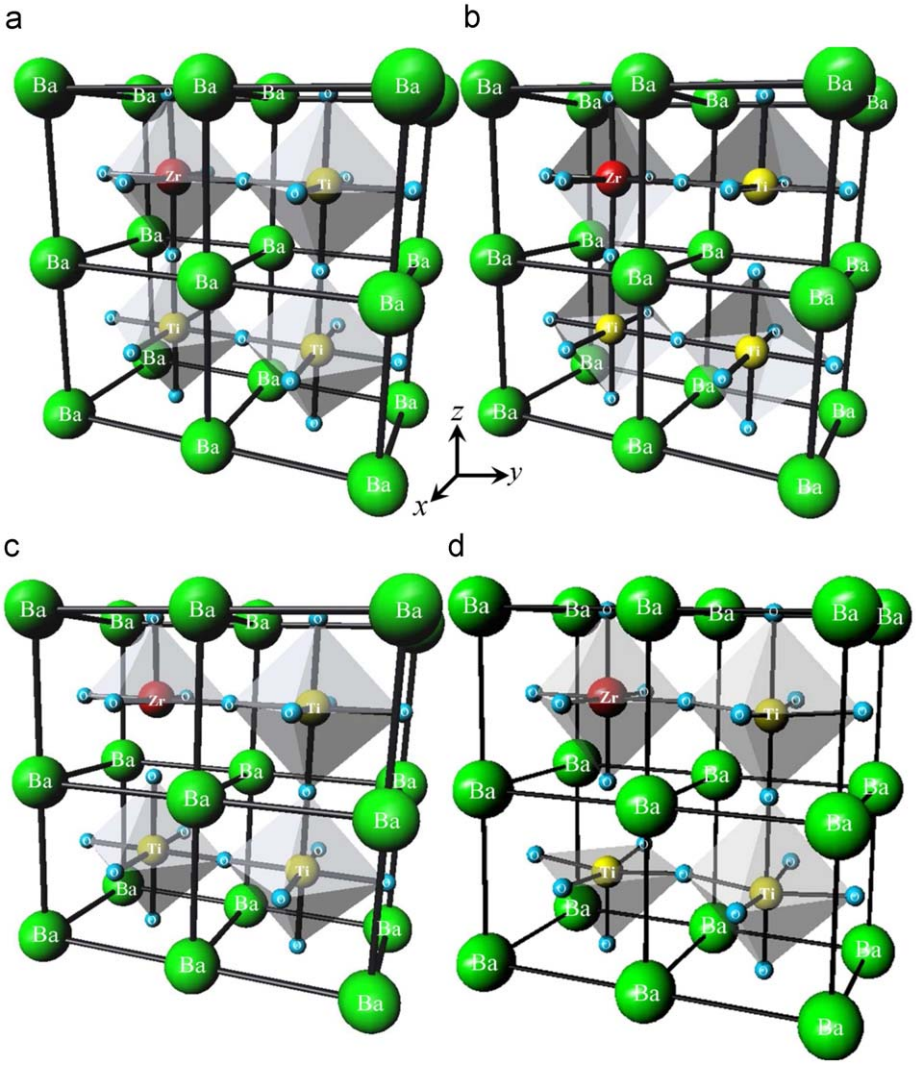

Fig. 2. Supercell representation 1 × 2 × 2 of the cubic BZT structure: (a) crystalline BZT-o, (b) ordered–disordered BZT-d_{Ti}; (c) ordered–disordered BTZ-d_{Zr} and (d) distorted BZT-d_{Ti}.

In this table, it was verified that the lattice parameter values of BZT powders are very close to that reported in the literature [39–41]. The slight differences can be related to the small lattice distortions caused by the residual stresses induced by the preparation conditions, mainly including heat treatment temperature, processing time and stages of grinding (in SSR).

3.2. Models: ordered, ordered–disordered and distorted for $Ba(Zr_{0.25}Ti_{0.75})O_3$

Figs. 2(a–d) show the schematic representation of four BZT supercells ($1 \times 2 \times 2$).

In an ordered BZT supercell, all Zr and Ti atoms are bonded to six oxygens ($[ZrO_6]$ and $[TiO_6]$ clusters), forming a polyhedron-type with octahedral configuration (Fig. 2(a)). This crystalline structure is characterized by a high degree of symmetry, i.e., without the presence of structural defects (oxygen vacancies or distortions) able to change the clusters organization. However, the ordered–disordered BZT supercells present a symmetry break along the O–Zr–O and/or O–Ti–O bonds, resulting in complex clusters with different coordination numbers ($[TiO_6]$–$[ZrO_6]$, $[TiO_6]$–$[ZrO_5]$ and $[TiO_5]$–$[ZrO_6]$) or distortions on the $[TiO_6]$–$[TiO_6]$ octahedral clusters (Figs. 2(b–d)). The presence of these complex clusters into the lattice can be detected by X-ray absorption near edge structure/extended X-ray absorption fine structure techniques and associated with quantum mechanical calculations [43,44].

Figs. 2(b–d) show a schematic representation of one perovskite-type cubic supercells with structural order–disorder caused by a displacement on Ti–O bonds (BZT-d_{Ti}), Zr–O bonds (BZT-d_{Zr}) and Ti–O bonds (BZT-d_{Ti}), respectively. In these models, it was performed a displaced along the [0 0 1] and [0 0 $\bar{1}$] direction (z-axis) on one Ti or Zr atom in order to represent the two Ti/Zr environments, i.e., $[Zr, TiO_5 \cdot V_O^z]$ complex clusters with pyramidal-type configuration, where $V_O^z = V_O^x$, $V_O^{\bullet}$, $V_O^{\bullet\bullet}$ and/or $[Ti, ZrO_6]$ with octahedral-type configuration.

Thus, these proposed models can be extended to n-clusters in a random distribution into the lattice. The structural defects observed in these supercells can be attributed to the oxygen vacancies and/or distortions, which present three different charge states: (a) neutral (V_O^x)—capture two electrons, (b) singly ionized ($V_O^{\bullet}$)—capture only one electron and (c) double ionized ($V_O^{\bullet\bullet}$)—it is not able to trap electrons. Double charged oxygen vacancies ($V_O^{\bullet\bullet}$) are the most mobile charge carriers into a structure, assuming an important role in the conduction mechanism.

3.3. Ultraviolet–visible absorption spectroscopy analyses

Figs. 3(a,b) show the UV–vis absorbance spectra of BZT powders prepared by PPM and SSR.

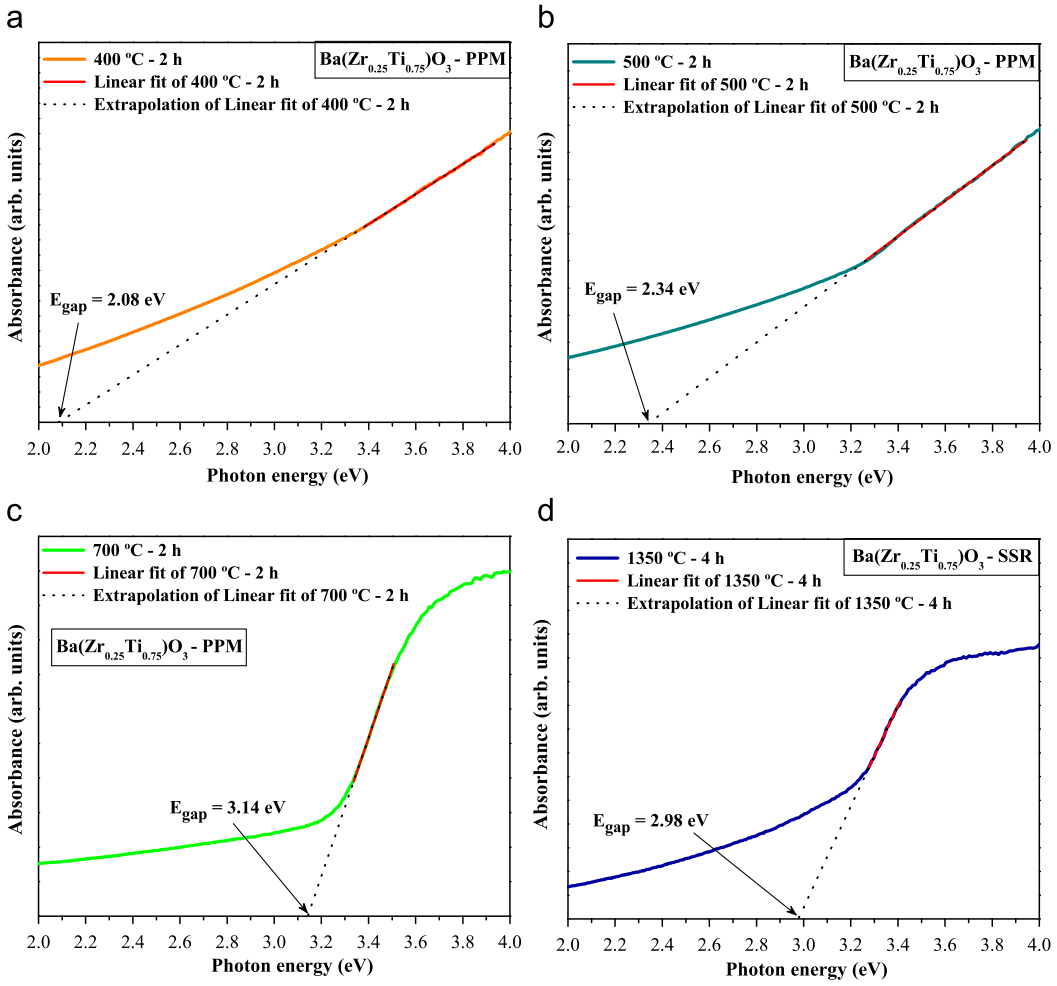

Fig. 3. (a) UV–vis absorbance spectra of BZT powders prepared by PPM and heat treated at (a) 400 °C, (b) 500 °C, (c) 700 °C for 2 h and (b) UV–vis absorbance spectra of BZT powders prepared by SSR heat treated at 1350 °C for 2 h.

The optical band gap energy (E_{gap}) was estimated by the method proposed by Wood and Tauc [45]. According to these authors the optical band gap is associated with absorbance and photon energy by the following equation:

$$h\nu\alpha \propto (h\nu - E_{gap})^2, \quad (1)$$

where α is the absorbance, h is the Planck constant, ν is the frequency and E_{gap} is the optical band gap.

In this case, the E_{gap} of BZT powders were evaluated extrapolating the linear portion of the curve or tail. In Figs. 3(a–c), the results indicate a considerable increase in the E_{gap} values with the temperature evolution for the BZT powders prepared by PPM. In principle, this behavior indicates the existence of different intermediary energy levels within the band gap of these materials, which can be arising from the structural order–disorder into the lattice due to a symmetry break between the O–Zr–O and O–Ti–O bonds (oxygen vacancies). Thus, the increase of heat treatment temperature is able to induce a structural rearrangement, reducing the presence of these energy levels within the band gap and increasing the E_{gap} values. Based on this hypothesis, we believe that the intermediary energy levels are composed of deep and shallow holes [46]. The deep holes (between the valence band and conduction band with small E_{gap} values) are considered emission centers responsible for the green, yellow, orange and red PL at room temperature, while the shallow holes (between the valence band and conduction band with high E_{gap} values) are associated to the violet and blue emissions.

An analysis performed on the results in Fig. 3(d) indicates that the E_{gap} of BZT powders prepared by PPM at 700 °C for 2 h is higher than by SSR at 1350 °C for 4 h. Based on this information, it is possible to conclude that the SSR resulted in a lower concentration of intermediary energy levels within band gap. In fact, although the repeated cycles of grinding in SSR are able to cause the formation of a high density of structural defects (distortions) into the lattice, the high heat treatment temperature for long processing time tends to minimize them. Therefore, this result indicates that the E_{gap} can be influenced by the preparation methods, mainly considering the experimental synthesis conditions (temperature, time, etc.) [47].

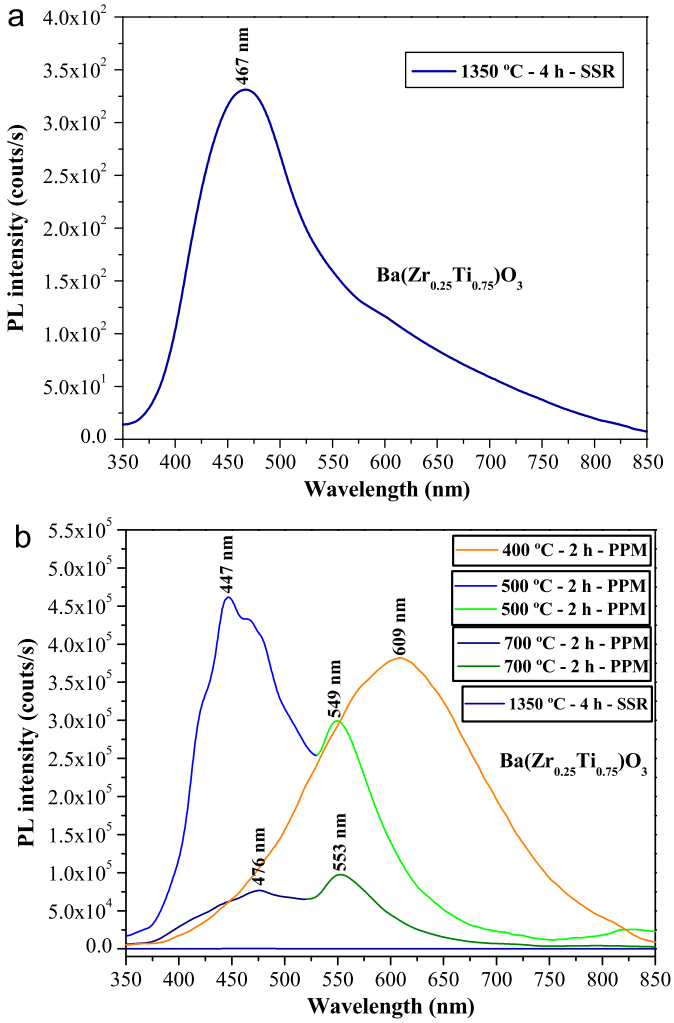

Fig. 4. (a) PL spectra of BZT powders prepared by SSR and heat treated at 1350 °C for 2 h and (b) PL spectra of BZT powders prepared by PPM and heat treated at 400, 500 and 700 °C for 2 h.

3.4. Photoluminescence analyses: emission spectra studies

Figs. 4(a,b) show the PL spectra of BZT powders prepared by PPM and SSR.

The PL profiles of BZT powders as a function of heat treatment temperature suggest an emission mechanism characterized by the participation of several energy levels (or light emission centers) able to trap electrons within the band gap (Figs. 4(a,b)). In Fig. 4(a), the powders prepared by SSR at 1350 °C for 4 h exhibited a low and broad PL emission, where the maximum is situated at around 467 nm (blue emission). This behavior suggests that there is a greater contribution of the shallow holes than the deep holes on the PL spectrum. On the other hand, the PL spectra of BZT powders formed by PPM are very different when compared to that obtained by SSR. In this case, considering the PPM, it was noted that the powder heat treated at 400 °C for 2 h presented a broad PL band with a maximum emission at around 609 nm (orange emission). As observed in the XRD patterns, this powder is in amorphous state or disordered at long range (Fig. 1(a)). However, the PL behavior indicates that there is a structural order at medium range, where the intermediary energy levels responsible for this optical property are arising from $[BaO_{12}]$, $[TiO_6]$ and $[ZrO_6]$ complex clusters.

The heat treatment performed at 500 °C for 2 h resulted in the presence of two well-defined broad PL bands. The first one was observed at 447 nm (blue emission), while the second one was verified at 549 nm (green emission) (Figs. 4(a,b)). Moreover, the presence of $BaCO_3$ in this powder was detected (Fig. 1(a)), as consequence of a reductive atmosphere arising from the organic matter decomposition ($C_2H_6O_2$ and $C_6H_8O_7$). According to the literature [48], the $BaCO_3$ does not present PL emission at room temperature. In addition, beyond this secondary phase, the temperature of 500 °C possibly resulted in favorable thermodynamic conditions to induce a rearrangement process between the $[BaO_{12}]$, $[TiO_6]$ and $[ZrO_6]$ complex clusters to form the BZT phase. Therefore, we believe that this mechanism causes a reorganization of the intermediary energy levels (deep and shallow holes) within the band gap, resulting in the formation of these two emission bands. Basically, the origin of these energy levels is associated with the symmetry break into the lattice due to the existence of oxygen vacancies or distortions, i.e., $[TiO_6]-[ZrO_5 \cdot V_O^z]$, $[TiO_6]-[TiO_5 \cdot V_O^z]$ complex clusters and/or distorted $[TiO_6]-[TiO_6]$ clusters (Figs. 2(b–d)).

When the powders were submitted to a heat treatment temperature of 700 °C, it was possible to verify a significant reduction in the PL intensity as well as a shifting of the maximum emission bands (Fig. 4(b)). A plausible explication for this phenomenon can be the increase of structural order or crystallinity of the material, consequently decreasing the oxygen

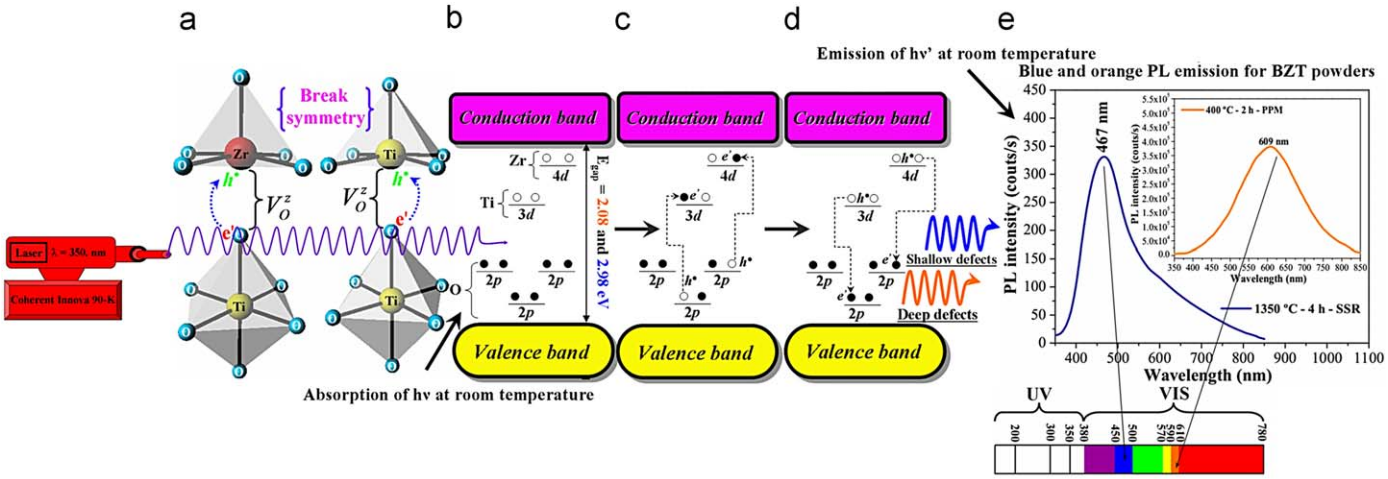

Fig. 5. (a) Interaction between laser wavelength and the $[ZrO_5]-[TiO_6]$ and/or $[TiO_5]-[TiO_6]$ complex clusters in the lattice, (b) proposed wide band model with the presence of intermediary energy levels (oxygen 2p and titanium 3d or zirconium 4d) within the band gap, (c) formation of STEs, (d) recombination of $e'-h^{\bullet}$ pair and (e) PL spectrum of BZT powders obtained by PPM and SSR.

vacancies into the lattice and the intermediary energy levels within the band gap. Moreover, under this temperature condition, the PL profile indicates a considerable reduction of the energy states related to the shallow holes due to the low band intensity located at around 476 nm (blue emission). Considering this information, it is possible to conclude that there is a transition from ordered–disordered to ordered BZT structure.

3.5. Wide band model

Fig. 5 shows a proposed model in order to explain the PL behavior of these ceramic oxides.

Blasse and Grabmaier [49] reported that the PL emission arises from the radiative return to the ground state, phenomenon that is in concurrence with the non-radiative return to the ground state. In the non-radiative process, the energy of the excited state is used to excite the vibrations of the host lattice, i.e., heat the lattice. The radiative emission process occurs more easily if there are trapped electrons by holes within the band gap [50]. According to the literature [47], the complex clusters observed in ordered–disordered materials result in intermediary energy levels able to trap electrons. In our case, the charge transference process as well as the trapping of electrons occur from $[TiO_6]' \rightarrow [ZrO_5 \cdot V_O^z]$; $[TiO_6]' \rightarrow [TiO_5 \cdot V_O^z]$; $[ZrO_6]' \rightarrow [TiO_5 \cdot V_O^z]$ complex clusters or $e'-h^{\bullet}$ pairs into the BZT lattice, when excited with 350 wavelength (Fig. 5a). In terms of band structures, the symmetry break caused by these kind of clusters leads to the formation of intermediary energy levels composed of oxygen (O) 2p states (small $E_{gap} = 2.08$ eV; deep holes) as well as titanium (Ti) 3d and zirconium (Zr) 4d states (high $E_{gap} = 2.98$ ev; deep holes) (Fig. 5(b)). During the excitation process at room temperature, several electrons situated in O 2p states are promoted to Ti 3d states or Zr 4d states as consequence of the absorption of photons ($h\nu$). Consequently, this physical process induces the formation of self-trapped excitons (STEs), i.e., trapping of electrons (e') by holes ($h^{\bullet}$) (Fig. 5(c)). When the electrons move from higher (Ti 3d states or Zr 4d states) to lower (oxygen 2p states) energy levels occurs the emission of photons ($h\nu'$) (Fig. 5(d)). The distribution and joint contribution of these energy levels influence in the E_{gap} value and consequently in the PL behavior of the powders. Hence, the PL profiles of BZT powders prepared by PPM and SSR exhibit different characteristics when excited by the same wavelength (Fig. 5(e)).

4. Conclusions

In summary, BZT powders were synthesized by the PPM at different temperatures (400, 500 and 700 °C) for 2 h and by the SSR at 1350 °C for 4 h. XRD patterns confirmed that the crystalline powders obtained by the PPM at 700 °C and SSR at 1350 °C have a cubic structure. UV–vis absorption spectra indicated that the increase of E_{gap} values is caused by a reduction of the deep increase of shallow holes between valence band and conduction band. The origin of these energy levels was associated to the structural order–disorder into the lattice due to a symmetry break between the O–Zr–O and O–Ti–O bonds, i.e., formation of $[TiO_6]-[ZrO_5 \cdot V_O^z]$; $[TiO_6]-[TiO_5 \cdot V_O^z]$ and $[ZrO_6]-[TiO_5 \cdot V_O^z]$ complex clusters (oxygen vacancies). The PL profiles of BZT powders prepared by the PPM and SSR showed significant differences when compared. These results suggest that the experimental conditions (heat treatment temperature, processing time) employed in the synthesis methods are key factors on the PL behavior. Moreover, the reduction observed in the PL intensity from 500 to 700 °C of BZT powders prepared by the PPM was related to the increase of structural organization. In this case, the defects associated to the oxygen vacancies were minimized into the lattice as well as the intermediary energy level distribution within the band gap. A model was proposed in order to explain the origin of the PL behavior, which was based on the existence of deep holes that are responsible by green–orange PL emission and shallow holes to blue PL emission.

Acknowledgments

The authors thank the financial support of the Brazilian research financing institutions: CAPES, CNPq and FAPESP.

References

[1] W. Chaisan, R. Yimnirun, S. Ananta, D.P. Cann, Mater. Lett. 59 (2005) 3732.
[2] M. Adamczyk, Z. Ujma, L. Szymczak, A. Soszynski, J. Koperski, Mater. Sci. Eng. B 136 (2007) 170.
[3] P. Kumar, S. Singh, J.K. Juneja, C. Prakash, K.K. Raina, Physica B 404 (2009) 1752.
[4] H. Fu, R.E. Cohen, Nature 403 (2000) 281.
[5] H. Lu, H. Chen, W. Li, B. Li, Fuel 83 (2004) 39.
[6] T. Maiti, R. Guo, A.S. Bhalla, J. Am. Ceram. Soc. 91 (2008) 1769.
[7] X. Wang, A. Yang, J. Phys. D 42 (2009) 075419.
[8] S.J. Kuang, X.G. Tang, L.Y. Li, Y.P. Jiang, Q.X. Liu, Scripta Mater. 61 (2009) 68.

[9] O.P. Thakur, C. Prakash, A.R. James, J. Alloys Compd. 470 (2009) 548.
[10] B.L. Cheng, C. Wang, S.Y. Wang, H.B. Lu, Y.L. Zhou, Z.H. Chen, G.Z. Yang, J. European Ceram. Soc. 25 (2005) 2295.
[11] J. Zhai, C. Gao, X. Yao, Z. Xu, H. Chen, Ceram. Inter. 34 (2008) 905.
[12] H. Chen, C. Yang, J. Zhang, B. Wang, H. Ji, Appl. Surf. Sci. 255 (2009) 4585.
[13] A. Hardy, A.S.V. Elshocht, W. Knaepen, J. D'Haen, T. Conard, B. Brijs, W. Vandervorst, G. Pourtois, J. Kittl, C. Detavernier, M. Heyns, M.K.V. Bael, H.V.D. Rul, J. Mullens, J. Mater. Chem. 19 (2009) 1115.
[14] L.G.A. Marques, L.S. Cavalcante, A.Z. Simões, F.M. Pontes, L.S. Santos-Júnior, M.R.M.C. Santos, I.L.V. Rosa, J.A. Varela, E. Longo, Mater. Chem. Phys. 105 (2007) 293.
[15] X.P. Jiang, M. Zeng, H.L.W. Chan, C.L. Choy, Mater. Sci. Eng. A 438–440 (2006) 198.
[16] X.G. Tang, K.H. Chew, H.L.W. Chan, Acta Mater. 52 (2004) 5177.
[17] N. Nanakorn, P. Jalupoom, N. Vaneesorn, A. Thanaboonsombut, Ceram. Inter. 34 (2008) 779.
[18] W. Cai, C. Fu, J. Gao, H. Chen, J. Alloys Compd. 480 (2009) 870.
[19] W. Cao, J. Xiong, J. Sun, Mater. Chem. Phys. 106 (2007) 338.
[20] X. Chou, J. Zhai, X. Yao, Mater. Chem. Phys. 109 (2008) 125.
[21] S.E. Hao, L. Sun, J.X. Huang, Mater. Chem. Phys. 109 (2008) 45.
[22] T. Badapanda, S.K. Rout, S. Panigrahi, T.P. Sinha, Curr. Appl. Phys. 9 (2009) 727.
[23] F. Moura, A.Z. Simões, L.S. Cavalcante, M. Zampieri, J.A. Varela, E. Longo, M.A. Zaghete, Appl. Phys. Lett. 92 (2008) 032905.
[24] C. Ostos, L. Mestres, M.L. Martínez-Sarrión, J.E. García, A. Albareda, R. Perez, Solid State Sci. 11 (2009) 1016.
[25] T. Maiti, R. Guo, A.S. Bhalla, J. Phys. D 40 (2007) 4355.
[26] B.W. Lee, S.B. Cho, J. European Ceram. Soc. 25 (2005) 2009.
[27] S.B. Reddy, K.P. Rao, M.S.R. Rao, Scripta Mater. 57 (2007) 591.
[28] W. Sakamoto, K.I. Mimura, T. Naka, T. Shimura, T. Yogo, J. Sol–Gel Sci. Technol. 42 (2007) 213.
[29] J. Xu, S. Shen, L. Gao, J. Zhai, X. Yao, Cryst. Growth. Des. 8 (2008) 1766.
[30] T. Maiti, E. Alberta, R. Guo, A.S. Bhalla, Mater. Lett. 60 (2006) 3861.
[31] T. Maiti, R. Guo, A.S. Bhalla, Appl. Phys. Lett. 90 (2007) 182901.
[32] T. Maiti, R. Guo, A.S. Bhalla, Appl. Phys. Lett. 89 (2006) 122909.
[33] J. Xu, C. Gao, J. Zhai, X. Yao, J. Xue, Z. Huang, J. Cryst. Growth 291 (2006) 130.
[34] A. Liu, J. Xue, X. Meng, J. Sun, Z. Huang, J. Chu, Appl. Surf. Sci. 254 (2008) 5660.
[35] M. Anicete-Santos, L.S. Cavalcante, E. Orhan, E.C. Paris, L.G.P. Simões, M.R. Joya, I.L.V. Rosa, P.R. de Lucena, M.R.M.C. Santos, L.S. Santos-Júnior, P.S. Pizani, E.R. Leite, J.A. Varela, E. Longo, Chem. Phys. 316 (2005) 260.
[36] L.S. Cavalcante, M.F.C. Gurgel, A.Z. Simões, E. Longo, J.A. Varela, M.R. Joya, P.S. Pizani, Appl. Phys. Lett. 90 (2007) 011901.
[37] C.D. Dimitrakopoulos, I. Kymissis, S. Purushothaman, D.A. Neumayer, P.R. Duncombe, R.B. Laibowitz, Adv. Mater. 11 (1999) 1372.
[38] M. Veith, S. Mathur, N. Lecerf, V. Huch, T. Decker, H.P. Beck, W. Eiser, R. Haberkorn, J. Sol–Gel Sci. Technol. 17 (2000) 145.
[39] Joint Committee on Powder Diffraction Standards. Diffraction Data File, no. 36-0019, International Centre for Diffraction Data (ICDD, formerly JCPDS), Newtown Square, PA, 2001.
[40] S. Mahajan, O.P. Thakura, D.K. Bhattacharya, K. Sreenivas, Mater. Chem. Phys. 112 (2008) 858.
[41] L.S. Cavalcante, M. Anicete-Santos, J.C. Sczancoski, L.G.P. Simões, M.R.M.C. Santos, J.A. Varela, P.S. Pizani, E. Longo, J. Phys. Chem. Solids 69 (2008) 1782.
[42] T.J.B. Holland, S.A.T. Redfern, Miner. Mag. 61 (1997) 65.
[43] V.M. Longo, A.T. de Figueiredo, S. de Lázaro, M.F. Gurgel, M.G.S. Costa, C.O. Paiva-Santos, J.A. Varela, E. Longo, V.R. Mastelaro, F.S. DE Vicente, A.C. Hernandes, R.W.A. Franco, J. Appl. Phys. 104 (2008) 023515.
[44] L.S. Cavalcante, J.C. Sczancoski, J.W.M. Espinosa, V.R. Mastelaro, A. Michalowicz, P.S. Pizani, F.S. De Vicente, M.S. Li, J.A. Varela, E. Longo, J. Alloys Compd. 471 (2009) 253.
[45] D.L. Wood, J. Tauc, Phys. Rev. B 5 (1972) 3144.
[46] L.S. Cavalcante, J.C. Sczancoski, F.S. De Vicente, M.T. Fabbro, M.S. Li, J.A. Varela, E. Longo, J. Sol-Gel Sci. Technol 49 (2009) 35.
[47] L.S. Cavalcante, M.F.C. Gurgel, E.C. Paris, A.Z. Simões, M.R. Joya, J.A. Varela, P.S. Pizani, E. Longo, Act. Mater. 55 (2007) 6416.
[48] M.L. Moreira, G.P. Mambrini, D.P. Volanti, E.R. Leite, M.O. Orlandi, P.S. Pizani, V.R. Mastelaro, C.O. Paiva-Santos, E. Longo, J.A. Varela, Chem. Mater. 20 (2008) 5381.
[49] G. Blasse, B.C. Grabmaier, Luminescent Materials, Springer, Berlin, 1994.
[50] E. Orhan, M. Anicete-Santos, M.A.M.A. Maurera, F.M. Pontes, C.O. Paiva-Santos, A.G. Souza, J.A. Varela, P.S. Pizani, E. Longo, Chem. Phys. 312 (2005) 1.